A New Anatomical Landmark for Reliable Identification of Human Area V5/MT: a Quantitative Analysis of Sulcal Patterning

Serge O. Dumoulin[1,2], Richard G. Bittar[1], Noor J. Kabani[1], Curtis L. Baker Jr[3], Georges Le Goualher[1], G. Bruce Pike[1] and Alan C. Evans[1]

[1]McConnell Brain Imaging Centre, Montréal Neurological Institute, McGill University, Montréal, Canada, [2]Utrecht University, Utrecht, The Netherlands and [3]McGill Vision Research Unit, Department of Ophthalmology, McGill University, Montréal, Canada

The location of human area V5 (or MT) has been correlated with the intersection of the ascending limb of the inferior temporal sulcus (ALITS) and the lateral occipital sulcus (LO). This study was undertaken to attempt a replication and quantification of these observations using functional magnetic resonance imaging. V5 was significantly activated in 19 hemispheres with alternating, low contrast, random checkerboard patterns. We confirmed the stereotaxic location of V5 and were able to describe a fairly consistent sulcal pattern in the parieto-temporo-occipital cortex. V5 was usually (95%) buried within a sulcus, most commonly within the inferior temporal sulcus (ITS) (11%), the ascending limb of the ITS (ALITS) (53%) and the posterior continuation of the ITS (26%). The average distance from V5 of two identified anatomical landmarks of V5, the junctions of the LO and the ALITS, and the ITS and ALITS, were both ~1 cm. However, the LO–ALITS junction often had to be determined by interpolation (47%), and was not always present even with interpolation (21%). In contrast, the ITS–ALITS junction was always present and V5 was usually (90%) located in a sulcus intersecting with this junction, making it a more reliable landmark for localizing V5 with respect to gross morphological features on individual cortical surfaces.

Introduction

The cerebral cortex consists of separate cortical areas involved in different processes, a phenomenon known as functional specialization. This functional specialization is presumed to be closely associated with the cytoarchitecture of the cortex (Brodmann, 1909; Roland and Zilles, 1998). However, there is considerable debate regarding the extent to which cortical gyri and sulci reflect this functional specialization. Only for primary cortices is such a relationship with gross anatomical features reasonably established (Stensaas et al., 1974; Rademacher et al., 1993; Gilissen and Zilles, 1996); for secondary and higher order cortices such a relationship remains unclear. Knowledge about such a relationship, and the extent of its variation, would especially have implications for the field of neuroimaging and brain mapping (Rademacher et al., 1993; Hunton et al., 1996). In this field, inter-subject data are commonly presented, compared and averaged in a standardized space (Talairach and Tournoux, 1988). To do this one has to know the variability of functional areas in the standard space (Watson et al., 1993; Hasnain et al., 1998). Variations of individual data sets in the standardized space of Talairach and Tournoux are due to gross anatomical variations, variations between gross anatomy and functional areas, and methodological differences (Steinmetz et al., 1989, 1990, 1991; Hunton et al., 1996). In this paper the relationship of a functionally defined visual area to gross anatomical structures on individual cortical surfaces is examined, thereby separating the variability due to gross anatomical variations, and variations between gross anatomy and functional areas.

Functional specialization within the human visual cortex was demonstrated by Zeki et al. (Zeki et al., 1991), who used positron emission tomography (PET) to demarcate cortical areas V4 and V5 (or MT), which they implicated in the processing of color and motion information respectively. In a further PET study, Watson et al. more accurately defined the location of V5 on the ventrolateral occipital cortex, slightly posterior to the junction of the ascending limb of the inferior temporal sulcus (ALITS) and the lateral occipital sulcus (LO) (Watson et al., 1993). Tootell et al. (Tootell et al., 1995) studied V5 in humans with functional magnetic resonance imaging (fMRI), and described a similar location in the standard (stereotaxic) space of Talairach and Tournoux (Talairach and Tournoux, 1988). However, they could not discern a consistent relationship between the region of V5 activation and the sulcal and gyral pattern in this region, except to observe that the activation was usually (but not always) buried within a shallow sulcus, as described by Watson et al. (Watson et al., 1993).

The parieto-temporo-occipital cortex is one of the most extensively gyrified regions of the cerebral cortex (Zilles et al., 1988), and consequently a high percentage of its surface area is buried within sulci. In addition, the sulcal and gyral pattern in this region is highly variable, evidenced by numerous alternative descriptions and nomenclature systems over the past century, either in relationship with V5 (Watson et al., 1993; Howard et al., 1995; McCarthy et al. 1995; Anderson et al., 1996) or without (Talairach and Tournoux, 1988; DeArmond et al., 1989; Ono et al., 1990; Carpenter, 1991; Duvernoy 1991; Nolte, 1999).

Since a consistent location of V5 in stereotaxic (Talairach) space has been indicated by several previous studies (Zeki et al., 1991; Watson et al., 1993; De Jong et al., 1994; Dupont et al., 1994; McCarthy et al., 1995; Tootell et al., 1995; Anderson et al., 1996; Uusitalo et al., 1997; Shulman et al., 1998), the goal of this study was to describe precisely the location of V5 with respect to the sulcal pattern in the lateral parieto-temporo-occipital cortex, using a set of fully automated registration and sulci extraction techniques. The use of such anatomical methods should result in an improved description and more detailed quantification of this relationship. This study entailed choosing a visual stimulus to activate selectively area V5 with fMRI, and a careful examination and re-classification of the sulcal patterns and landmarks in this region.

Materials and Methods

fMRI Scanning

fMRI was performed in 15 normal subjects, 10 of whom showed significant activations [eight males, two females; one left handed, nine right handed; average age 31 years (range 24–44 years)]. All subjects had normal or corrected to normal acuity. These studies were conducted with the subjects lying on their back with a surface-coil (circularly polarized, receive only) centered over their occipital poles. The visual stimuli were presented on a rear-projection screen placed at the end of the bore of the magnet, which was viewed by means of a mirror mounted above the eyes

at an angle of ~45°. Head position was fixed by a foam headrest and either by the use of a bite-bar or by a combination of immobilizing hearing protectors and a bar pressing on the bridge of the subject's nose. These constraints reduced head motion and virtually eliminated cumulative head drift during the scanning session.

Multislice T2*-weighted gradient echo (GE) echo-planar imaging images (TR = 3.0 s, TE = 51 ms, flip angle = 90°) were acquired with a Siemens Magnetom Vision 1.5T MRI. A 128 × 128 acquisition matrix was acquired with a 300 × 300 mm rectangular field of view. For this study, 10–12 contiguous 4–6 mm slices were obtained parallel to the calcarine sulcus, and care was taken to include the junction of the inferior temporal sulcus (ITS) and the ALITS. One hundred and twenty measurements (time frames) were acquired, giving a total scanning time of 6 min per dynamic scan. Baseline and activation conditions were alternated every 45 s, resulting in four activation periods and four baseline periods per dynamic scan. Two to four dynamic scans were performed in each session.

Anatomical MRI Scanning

T1-weighted anatomical MRI (aMRI) images were acquired with the surface-coil in place, prior to the commencement of the functional scans. Thus, if no head movement occurred, the anatomical and functional surface-coil MRI images were aligned. This aMRI utilized a 3-D GE sequence (TR = 22 ms, TE = 10 ms, flip angle 30°) and yielded ~80 256 × 256 sagittal images with a thickness of 2 mm. The signal intensity of a surface-coil aMRI decreases as a function of the distance from the coil. This intensity gradient interferes with most of the automatic algorithms used. Therefore, in all subjects, T1-weighted global MRI images were acquired with a head-coil (circularly polarized, transmit and receive), also using a 3-D GE sequence, yielding ~170 256 × 256 sagittal images comprising 1 mm^3 voxels. The surface-coil aMRI was aligned with the head-coil scan, thereby allowing an alignment of the functional data with a head-coil aMRI. All studies were performed with the informed consent of the subjects and were approved by the Montreal Neurological Institute Research Ethics Committee.

Visual Stimulus

The visual stimulus was generated on a Macintosh Powerbook 160 using a modified program from the Video Toolbox (Pelli, 1997), and displayed with an LCD projector (NEC-MT). The visual display was 36 cm in both height and width, corresponding to 15° at a viewing distance of 135 cm. The activation condition consisted of random checkerboard patterns (see Fig. 1), which were replaced by fresh random checkerboard patterns at a frequency of ~2 Hz, i.e. two checkerboard patterns per second. Each check of the checkerboard pattern subtended ~0.06°, and was randomly assigned a lighter (L_{max}) or darker (L_{min}) luminance value than the mean background luminance (435 cd/m^2). The contrast, defined as (L_{max} − L_{min})/(L_{max} + L_{min}), was 3%. The baseline condition comprised a stationary random checkerboard pattern, otherwise identical to that in the activation condition. A black fixation dot (0.3°) was affixed to the center of the visual display.

Area V5 receives a dominant input from the magnocellular stream, making it relatively insensitive to a reduction of contrast compared with other cortical areas (Tootell *et al.*, 1995; Anderson *et al.*, 1996) [for non-human primate studies see (DeYoe and Van Essen, 1988; Maunsell *et al.*, 1990; Sclar *et al.*, 1990; Cheng *et al.*, 1994)]. Temporal modulation (flicker), i.e. the alternation of the random checkerboard patterns, elicits a response from V5 (Tootell *et al.*, 1995) [for animal studies see also (Lagea *et al.*, 1994)] while suppressing eye-tracking movements which can also activate V5 and related areas (Barton *et al.*, 1996; Freitag *et al.*, 1998). The above-mentioned arguments indicate a selective V5 activation by the visual stimulus used.

Data Analysis

The images were analyzed on SGI workstations using purpose-built software developed in the Neuroimaging Laboratory at the Montreal Neurological Institute. The global aMRI scans were corrected for intensity non-uniformity (Sled *et al.*, 1998) and automatically registered (Collins *et al.*, 1994) into a stereotaxic space (Talairach and Tournoux, 1988) using a stereotaxic average model of 305 brains (Evans *et al.*, 1992). The surface-coil anatomical scans were aligned with the head-coil anatomical
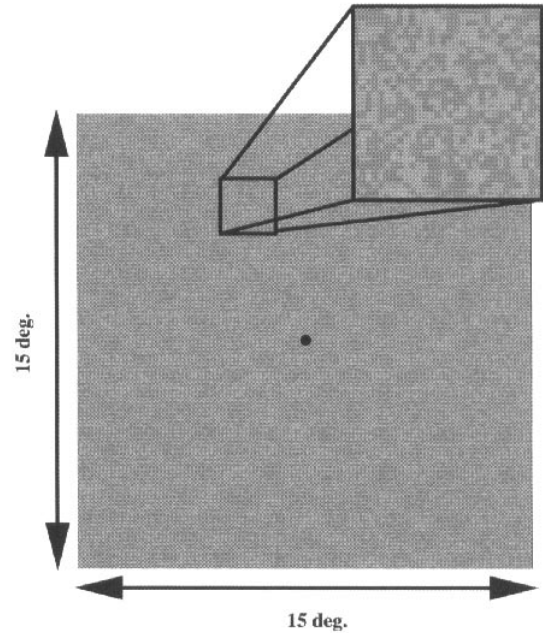

Figure 1. One frame of a random checkerboard pattern. Each check is randomly assigned a darker or lighter value than the mean luminance.

scans using an automated script combining correction for the intensity gradient (Sled *et al.*, 1998) and intra-subject registration (Collins *et al.*, 1994; Maes *et al.*, 1997). The functional data were blurred with a 3-D full-width–half-maximum (fwhm) filter of 6 mm to increase signal-to-noise by attenuating high frequency noise, and analyzed using a Spearman rank order statistical test for each voxel. The acquired *t*-statistic map was transformed into the standard Talairach space by combining the transformation files from the previous two steps. Only *t*-statistical maps with a group of adjacent voxels whose *t*-statistical values corresponded, after correcting for multiple comparisons, to *P*-statistical values smaller than 0.001 (*t* = 5.4) were included in this study. Using the *P* < 0.001 criterion, regions of activations were identified. The location of V5 has been correlated with the parieto-temporo-occipital cortex (Zeki *et al.*, 1991; Watson *et al.*, 1993; McCarthy *et al.*, 1995; Tootell *et al.*, 1995); therefore, the location of the voxel with the most significant *t*-statistical value in this region was taken to be V5. This identification process of V5 was similar to that used by Watson *et al.* (Watson *et al.*, 1993). Sulcal regions were identified using automated algorithms which extract the cortical surface (MacDonald *et al.*, 1994, 1998) and then identify sulcal zones using curvature criteria (Le Goualher *et al.*, 1996, 1998). Those in the region of interest were manually identified (Ono *et al.*, 1990), using a 3-D interactive display program (MacDonald, 1996). The voxels with the *t*-statistical values above a certain threshold and all sulci were displayed on an extracted cortical surface (MacDonald *et al.*, 1994, 1998). Cortical unfolding was then performed to aid the visualization of functional activation deep within the sulci (MacDonald, 1998).

Identification of Sulci

The anatomical MRI images were initially examined in the sagittal plane for major sulci (Fig. 2). The Sylvian fissure and the superior temporal sulcus were identified, followed by the often discontinuous ITS, running parallel to the above-mentioned sulci. The posterior end of the ITS was traced to the formation of the ventrodorsally oriented sulcus, which has been previously referred to as the ALITS (Watson *et al.*, 1993). At this junction, the ITS usually extended horizontally into the occipital lobe, and when it did not reach the occipital pole we labeled it the posterior continuation of the ITS (PCITS). In cases where this horizontal sulcus reached the occipital pole it was termed the posterior continuation/lateral occipital sulcus (PCITS/LO). Often there was a horizontal sulcus
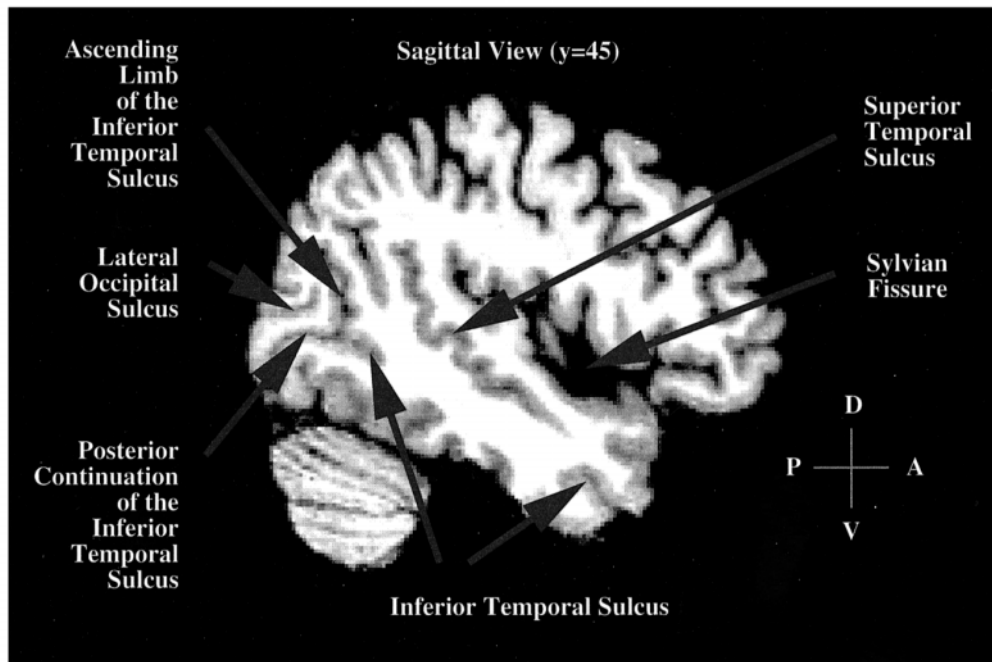
Figure 2. A sagittal view of a brain in stereotaxic space. The sulci of interest are indicated.

dorsal to the PCITS or PCITS/LO, which extended to the occipital pole, the LO (Ono *et al.*, 1990).

Results

Area V5

The acquired *t*-statistical map contained several *t*-statistical peaks. The *P* < 0.001 criterion usually revealed only one activation region in each hemisphere, situated in the general location where V5 (or MT) has been previously reported, i.e. the parieto-temporo-occipital cortex (Zeki *et al.*, 1991; Watson *et al.*, 1993; De Jong *et al.*, 1994; Dupont *et al.*, 1994; Cheng *et al.*, 1995; McCarthy *et al.*, 1995; Tootell *et al.*, 1995; Uusitalo *et al.*, 1997; Shulman *et al.*, 1998). For examples see Figures 4 and 5*a*. In a few cases two activation points were found in the region of interest. These points, however, were always located within the same sulcus and could, based on the anatomical dimensions of V5 (Tootell and Taylor, 1995), still arise from the same area. The criterion sometimes revealed more activation points. These, however, had lower peak *t*-statistical values and were never located within the parieto-temporo-occipital cortex.

In five of our subjects no significant responses were observed. In three subjects, the highest *t*-statistical peaks were present in the region of interest but did not reach statistical significance due to our conservative statistical criteria (*P* > 0.001). In the other two cases a moving noise pattern, present through external interactions with the stimulus presentation, modulated the subject's attention and thus also the fMRI activity in area V5 (Beauchamp *et al.*, 1997; O'Craven *et al.*, 1997). This pattern was present throughout the scanning session and virtually eliminated the identification of V5 by our activation paradigm and statistical analysis.

The average coordinates and standard deviations in stereotaxic Talairach space of V5 for the left hemisphere ($x = -47 \pm 3.8$, $y = -76 \pm 4.9$, $z = 2 \pm 2.7$; $n = 10$) and for the right hemisphere
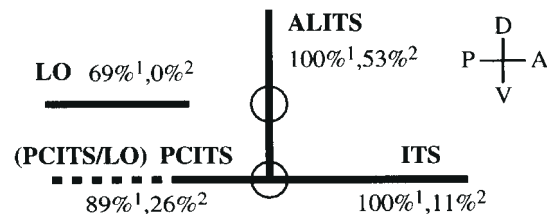
Figure 3. A generic model of the sulcal pattern in the parieto-temporo-occipital cortex. The percentages indicate the likelihood of each sulcus being present (1) and the likelihood of finding V5 within each sulcus (2); the latter does not add up to 100% because V5 was not always located within these sulci. The circles indicate two (interpolated) junctions.

($x = 44 \pm 3.3$, $y = -67 \pm 3.1$, $z = 0 \pm 5.1$; $n = 9$) were similar to the ones found by Watson *et al.* (Watson *et al.*, 1993) ($x = -41 \pm 5.6$, $y = -69 \pm 6.0$, $z = 2 \pm 5.3$ and $x = 41 \pm 3.7$, $y = -67 \pm 4.7$, $z = 2 \pm 3.2$ for the left and right hemisphere respectively; $n = 12$) and Tootell *et al.* (Tootell *et al.*, 1995) ($x = \pm 45 \pm 3.6$, $y = -76 \pm 7.5$, $z = 3 \pm 2.5$; $n = 6$) [see also (Zeki *et al.*, 1991; De Jong *et al.*, 1994; Dupont *et al.*, 1994; McCarthy *et al.*, 1995; Uusitalo *et al.*, 1997; Shulman *et al.*, 1998)]. No significant differences between the activation foci in the left and right hemispheres was observed with respect to the peak *t*-statistical values or the total volumes of significant activation (*P* > 0.05).

The Sulcal Pattern

We found a fairly consistent sulcal pattern in the region of interest (the parieto-temporo-occipital cortex), enabling us to describe a generic model of the sulcal pattern (Fig. 3). Variations in this model are produced by the absence or presence of the LO, the PCITS and the PCITS/LO. In all cases (19 hemispheres) the posterior end of the ITS gave rise to a roughly ventrodorsally oriented sulcus, the ALITS. At this junction the ITS extended pos-

teriorly in 89% (17/19) of the cases. This extension was in 47% (9/19) defined as the PCITS and in the remaining 42% (8/19) the PCITS/LO. The LO was identified in 69% (13/19). In 58% (11/19) the LO was located dorsal to the PCITS (37%) or PCITS/LO (21%) without a meeting point to either of the above-mentioned sulci. In the remaining 11% (2/19) the LO connected to the ALITS, in which case there was neither a PCITS nor a PCITS/LO.

The incidence rates (in %) of the sulci are similar to the ones described by Ono *et al.* (Ono *et al.*, 1990). Ono *et al.* were able to identify the ITS in 98% of the cases, though they did not specifically describe the ALITS. They described an occipital extension that typically became the lateral occipital sulcus (PCITS/LO 42%) in 34% of the cases and identified the lateral occipital sulcus (LO and PCITS/LO 89%) in 96%.

Relation of Area V5 to the Sulcal Pattern

In 95% of all cases, V5 was located within the depth of a sulcus. The one activation peak (5%) that was not located within a sulcus was positioned on the gyrus directly posterior to the ALITS. As shown in Figure 3, 53% of the activations were found in the ALITS, 11% in the ITS, and 26% in the PCITS and PCITS/LO (5% was located in the PCITS and 21% in the PCITS/LO). No activation peaks were found in the LO. The remaining location of V5 (5%) was in the descending limb of the superior temporal sulcus. Fourteen V5 locations are shown in Figures 4 and 5. In Figure 4 the *t*-statistical maps and labelled sulci are shown in a sagittal slice chosen to visualize both the V5 locations and labelled sulci. In Figure 5, the V5 locations are displayed on a cortical surface and an unfolded cortical surface. The unfolded surfaces are shown for the parieto-occipito-temporal junction. In the latter case, the identified sulci are displayed with different labels.

Landmarks

The average stereotaxic Talairach coordinates and standard deviations of two possible anatomical landmarks for the position of V5 were determined, i.e. the LO (and PCITS/LO) and ALITS (LO–ALITS) as defined by Watson *et al.* (Watson *et al.*, 1993) and the junction of the ITS and ALITS (ITS–ALITS) (see Fig. 5). These coordinates were $x = -47 \pm 3.5$, $y = -71 \pm 5.0$, $z = -2 \pm 3.7$ ($n = 10$) and $x = -45 \pm 3.2$, $y = -74 \pm 5.3$, $z = 2 \pm 3.4$ ($n = 8$) respectively for the left hemisphere. For the right hemisphere the respective coordinates were $x = 46 \pm 2.9$, $y = -66 \pm 5.8$, $z = -2 \pm 7.7$ ($n = 9$) and $x = 46 \pm 2.4$, $y = -63 \pm 4.1$, $z = 6 \pm 7.3$ ($n = 7$). As shown in Table 1, these landmarks were 4 ± 4.6 mm ($n = 8$) apart in the left hemisphere and 7 ± 6.5 mm ($n = 7$) apart in the right hemisphere.

The LO–ALITS junction could be determined in 79% (15/19) of the cases. It consisted in 42% (8/19) of an actual meeting point, of which 25% (2/8) was a meeting point between the LO and the ALITS, and the remaining 75% (6/8) was the meeting point between the PCITS/LO and the ALITS (see Figure 3 and Table 1). This last junction point, between the PCITS/LO and the ALITS, is identical to the ITS–ALITS meeting point (see Fig. 3). Where the LO and the ALITS did not intersect, their interpolated meeting point was determined (Watson *et al.*, 1993) by extending the LO anteriorly in line with its general orientation until it joined with the ALITS. Such an interpolated meeting point was

found in 53% (10/19) of the cases. When two LO–ALITS meeting points existed, i.e. both the LO and PCITS/LO were present in 16% (3/19) of the cases, the average between the two was taken. No LO–ALITS junction, either real or interpolated, could be determined in 21% (4/19) of all cases. The average distance and standard deviation between the LO–ALITS meeting point and the position of V5 was 7 ± 5.1 ($n = 8$) and 10 ± 6.2 mm ($n = 7$) for the left and the right hemisphere respectively.

The ITS–ALITS junction was present in all cases. For the ITS–ALITS junction this average distance corresponded to 9 ± 4.2 ($n = 10$) and 10 ± 5.1 mm ($n = 9$) for the left and right hemisphere respectively.

To estimate the variability of the position of V5, the distances from the individual V5 coordinates to the average V5 position were determined. The average absolute value of the distance and standard deviation were 6.4 ± 2.4 ($n = 10$) and 6.5 ± 2.8 mm ($n = 9$) for the left and right hemisphere respectively. To determine whether inter-subject registration of the anatomical landmarks would decrease the variability of the position of V5, the same distances were computed after substraction of the individual landmark coordinates from the corresponding coordinates of V5. These distances after subtraction of the ITS–ALITS coordinates were 6.3 ± 2.6 ($n = 10$) and 10.4 ± 5.0 mm ($n = 9$) for the left and right hemisphere respectively. The distances after substraction of the LO–ALITS coordinates were 6.6 ± 3.5 ($n = 8$) and 9.3 ± 4.2 mm ($n = 7$) for the left and right hemisphere respectively. None of these distances differ significantly from each other ($P > 0.05$).

Methodological Issues

The functional data were not corrected for head movement; however, the head restraints minimized motion. To estimate the amount of movement of a given point on the cortex, functional scans of six different subjects were analyzed with the AIR package (Woods *et al.*, 1992, 1998; Jiang *et al.*, 1995). The average amount of motion of a point on the surface of the brain was 0.27 mm ($n = 702$), with a maximum displacement of 1.1 mm. All these estimates were calculated with absolute values, i.e. the direction of motion was not taken into account and was assumed to always be the same. Therefore these estimates represent the worst case scenario.

The intra-subject registration error after transformation from the surface-coil aMRI to the head-coil aMRI was determined by selecting, in four subjects, six or seven specific anatomical landmark points in the head-coil aMRI and surface-coil aMRI. The landmark points of the surface-coil aMRI were mapped into the same space as the head-coil aMRI, both with the automatic procedure and by a landmark-based procedure. In the landmark-based procedure the distances between the surface-coil landmarks and the head-coil landmarks were minimized. The average distance and standard deviation between the landmark points of the head-coil aMRI and the corresponding ones of the surface-coil aMRI mapped into the same space through the landmark-based registration was 0.74 ± 0.43 mm ($n = 27$). The corresponding value for the automatic registration was 1.01 ± 0.96 mm ($n = 27$). These average values also contain the average identification error for the landmark points. Even though this difference in group mean is significant, we note that the landmark-based registration result is optimized for the given

Figure 4. The *t*-statistical map and the extracted and labeled sulci are superimposed on the anatomical MRI volumes of four subjects in stereotaxic space. The colorbar indicates the *t*-statistical values that are displayed. The ITS is labeled with yellow, the ALITS is labeled with green, and the PCITS, PCITS/LO and LO are labeled with blue, purple and red, respectively.
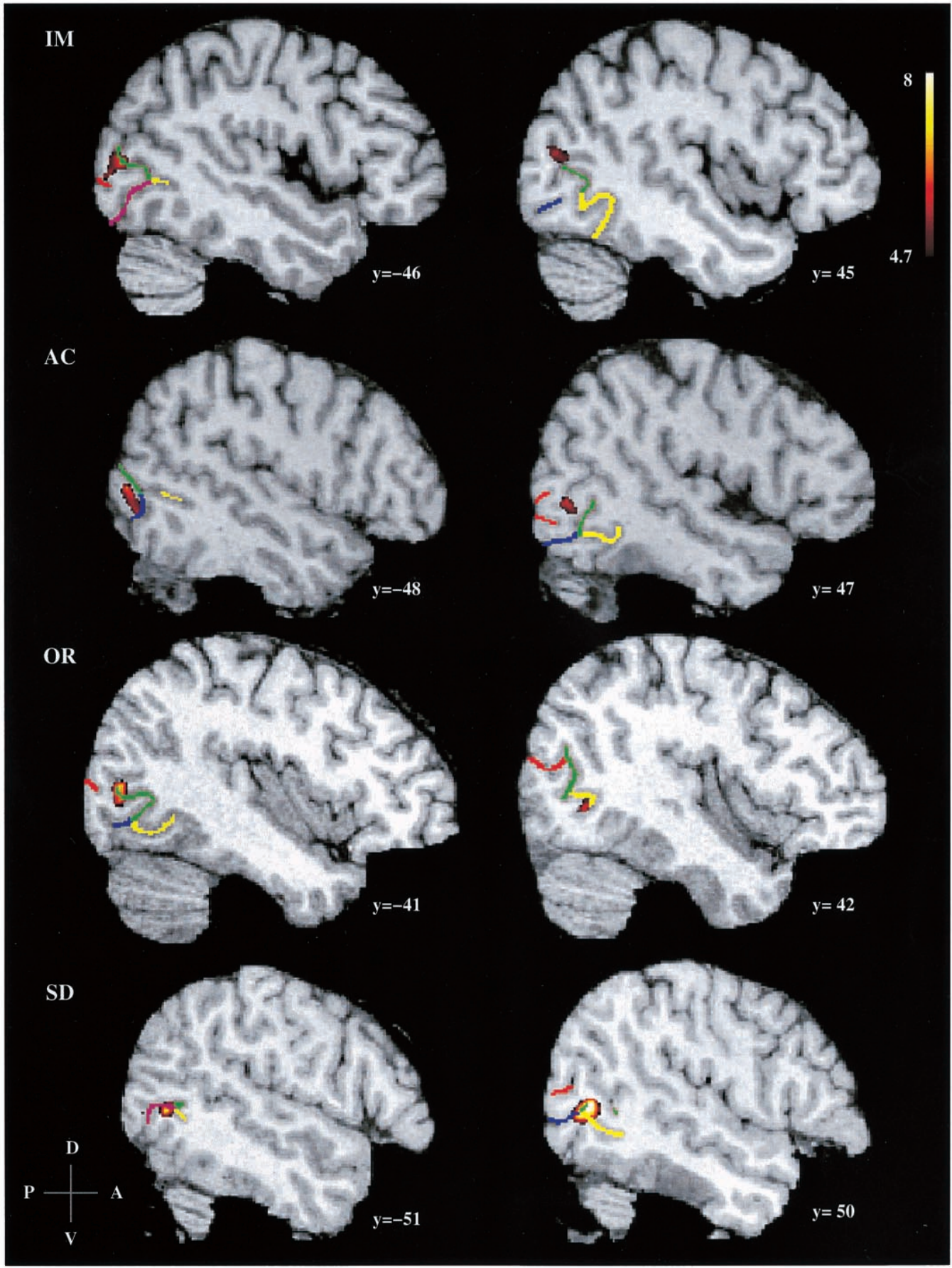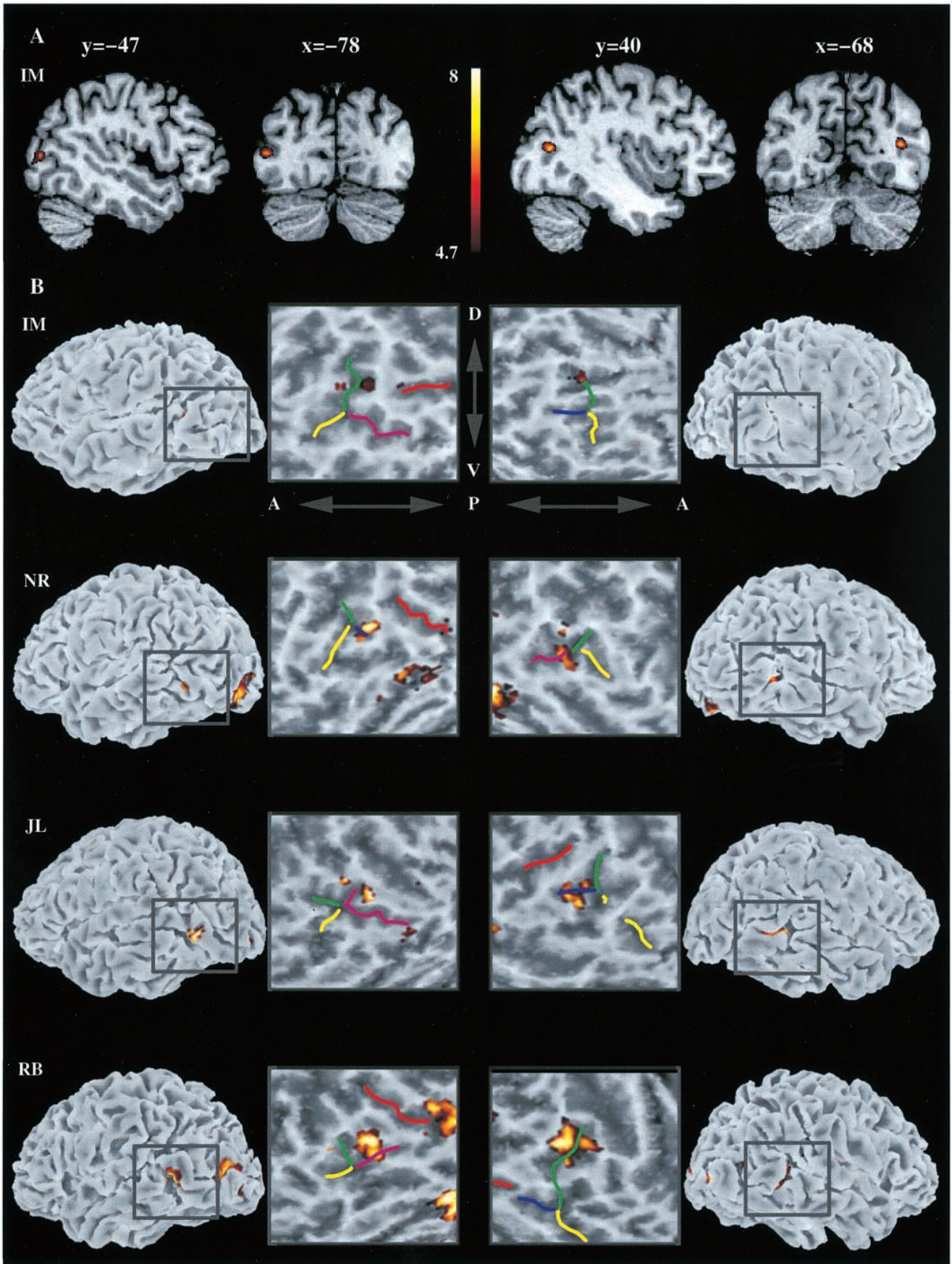
Table 1.
The distance from V5 to the junction points, ITS–ALITS and LO-ALITS, and the distance between the junction points

Subject	ITS–ALITS (mm)			LO–ALITS (mm)			Dist. junct. (mm)		
	L	R	L+R	L	R	L+R	L	R	L+R
1	3[1]	11		3[1,3]	2[1,3]		0	9	
2	5	2[1]		–	2[2]		–	0	
3	6	14		–	11[3]		–	15	
4	15	8		1[1,3]	20		6	17	
5	7	10		8[3]	10[2]		1	0	
7	14	11		14[2]	16[3]		0	3	
10	6	NS		1[1,3]	NS		6	NS	
11	15	19		15[3]	–		0	–	
13	6	2		10	7[3]		14	5	
15	8	10		7[4]	–		7	–	
Mean	9	10	9	7	10	8	4	7	6
SD	4.2	5.1	4.7	5.1	6.2	5.8	4.6	6.4	5.7
n	10	9	19	8	7	15	8	7	15

The junction points that fall within the significant V5 activation are marked with a 1, a LO-ALITS junction marked with a 2 is the intersection of the PCITS/LO and the ALITS, an interpolated junction is indicated with a 3, and 4 represents an average of two junctions (PCITS/LO and LO). NS is no significant activation.

set of landmarks. Therefore we conclude that the results for the automatic procedure are at least comparable to the manual landmark-based registration.

Discussion

Area V5
The position of V5 (or MT) in stereotaxic Talairach space as determined here is consistent with previous studies (Zeki *et al.*, 1991; Watson *et al.*, 1993; De Jong *et al.*, 1994; Dupont *et al.*, 1994; McCarthy *et al.*, 1995; Tootell *et al.*, 1995, Uusitalo *et al.*, 1997; Shulman *et al.*, 1998). In most cases, V5 was selectively activated, i.e. only one activation peak was determined in each hemisphere. This activation peak was always situated in the parieto-temporo-occipital cortex. In some cases other visual areas were also activated, though with lower *t*-statistical values. These activation sites were, based on their position, probably V3/V3A, VP and less often V1/V2 (Sereno *et al.*, 1995; DeYoe *et al.*, 1996; Tootell *et al.*, 1996; Engel *et al.*, 1997; Tootell *et al.*, 1997). These points were never located in the parieto-temporo-occipital cortex. This result is consistent with the notion that V5 receives its input mainly from the M-pathway and thus is relatively sensitive to low contrast and high temporal frequency (Tootell *et al.*, 1995).

Suppose, however, that there were a number of nearby areas, all M-cell driven and responsive to high temporal frequencies, but varying in relative strength of their activation in response to our stimulus. This situation would result in different areas being identified as V5 in different subjects; in some proportion of the cases, two or more spatially distinct *t*-statistical peaks would then be present in the region of interest. Such an outcome was never observed, except for a few cases where the distance be- tween the peaks, always located within the same sulci, was small enough to have been produced by the same V5 area (Tootell and Taylor, 1995). These results confirm the selectivity of this visual stimulus for eliciting V5 responses.

The Sulcal Pattern
The sulcal patterns on the lateral surface of the occipital lobe are variable, and its gyri are often simply referred to as lateral occipital gyri (DeArmond *et al.*, 1989; Carpenter, 1991; Nolte, 1999). Several different systematic descriptions have been given. One description distinguishes three occipital gyri, the inferior, middle (or lateral) and superior occipital (Talairach and Tournoux, 1988; Duvernoy, 1991). According to Duvernoy, these gyri are separated by the inferior and superior occipital sulci, and the inferior occipital sulcus is frequently absent (Duvernoy, 1991). In the latter case only two gyri can be distinguished. The lateral occipital sulcus is considered to be an intermediate sulcus subdividing the middle occipital gyrus (analogous to the middle frontal sulcus). Others only distinguish two gyri, the superior and lateral (or inferior) occipital (Chusid, 1973; DeGroot, 1991); however, the lateral occipital gyrus may have further subdivisions. These two gyri are separated by the lateral occipital sulcus, of which there are often two (Ono *et al.*, 1990). These lateral sulci (Ono *et al.*, 1990) correspond to Duvernoy's inferior and lateral occipital sulci. These sulci were of interest to our study as they are correlated with the location of V5 (Watson *et al.*, 1993). All horizontally oriented occipital sulci located in the vicinity of V5 were defined as the lateral occipital sulcus (Ono *et al.*, 1990). We differentiate between two types of lateral occipital sulci, the LO and the PCITS/LO. This distinction was based on the observation that the ITS often extended into the occipital lobe where it became the lateral occipital sulcus (PCITS/LO) (Ono *et al.*, 1990). This distinction proved useful because V5 was never located in one type, the LO, but was in some cases positioned in the PCITS/LO and sometimes in the PCITS. The posterior end of the highly interrupted ITS gave rise to a ventrodorsally oriented sulcus, the ALITS (Watson *et al.* 1993). This sulcus, which Duvernoy (Duvernoy, 1991) referred to as the anterior occipital sulcus, separates the occipital and temporal lobes. Watson *et al.* also referred to the ALITS as the posterior continuation of the inferior temporal sulcus. This is different from our definition of the PCITS, which is the horizontally oriented extension of the ITS that does not reach the occipital pole and therefore is not referred to as PCITS/LO. Thus the definitions of the sulci used in this paper (see Fig. 2) are consistent with most other descriptions given for the sulcal patterns in our region of interest.

Relation of Area V5 to the Sulcal Pattern
In agreement with the observations of Watson *et al.* (Watson *et al.*, 1993) and Tootell *et al.* (Tootell *et al.*, 1995), V5 was mostly found within a sulcus. This finding may be explained by the extensive gyrification in this area, i.e. relatively more cortex is buried within sulci (Zilles *et al.*, 1988; Tootell *et al.*, 1995). The sulcus in which V5 was located was variable but mainly limited to three sulci, i.e. ALITS, ITS and the posterior extension of the ITS (PCITS and PCITS/LO). V5 was most commonly located in the ALITS. Watson *et al.* found the position of V5 to be close to the junction point (actual or interpolated) of the lateral occipital sulcus (LO and PCITS/LO) and the ALITS (Watson *et al.*, 1993). Our results show that the position of V5 is located, on average,

Figure 5. (*A*) An anatomical MRI volume in stereotaxic space with the superimposed *t*-statistical map. The color bar indicates the *t*-statistical values that are displayed. (*B*) Locations of V5 displayed on the corresponding cortical and unfolded cortical surfaces. On the unfolded cortical surfaces the sulci of interest are labeled. The ITS is labeled with yellow, the ALITS is labeled with green, and the PCITS, PCITS/LO and LO are labeled with blue, purple and red, respectively.

1 cm from this junction point. This average distance to V5 is the same for another anatomical landmark, i.e. the junction between the ITS and the ALITS. Realignment of the results to either landmark did not significantly alter the variation of the V5 locations. However, the latter was always present in our study and interpolation was unnecessary. Also, V5 was usually located within a sulcus intersecting with this junction, making it a more reliable V5 landmark.

Methodological Issues

Misregistration between the functional and anatomical data could potentially be an explanation for the variability between those data. These potential registration errors may have their origin in two processes, both relating to the short (surface-coil) aMRI taken before each functional scanning session. This aMRI was assumed to be in the same position as the functional scans taken immediately afterwards. A potential source of a registration error could occur due to movement of the subject during the scanning session, thus making our assumption false. Though we did not correct for movement the head constraints minimized motion and virtually eliminated cumulative head drift. The absolute movement values for a point on the surface of a brain are (~30 times) smaller than the variations between functional and anatomical data. Other registration errors may occur due to misregistration of the surface-coil aMRI with the head-coil aMRI. However, these registration errors are also (~10 times) smaller than the variations of our data. Therefore we conclude that misregistration issues do not play a significant role in the explanations of our results.

Variable fMRI responses could also potentially be an explanation for the variability between functional and anatomical data. However, the reproducibility of fMRI results is very good (Ramsey *et al.*, 1996b; Casey *et al.*, 1998) and correlates highly with PET (Dettmers *et al.*, 1996; Ramsey *et al.*, 1996a). The reproducibility of the stereotaxic coordinates of area V5 has been indicated by several previous studies using a variety of imaging techniques (Zeki *et al.*, 1991; Watson *et al.*, 1993; De Jong *et al.*, 1994; Dupont *et al.*, 1994; McCarthy *et al.*, 1995; Tootell *et al.*, 1995; Anderson *et al.*, 1996; Uusitalo *et al.*, 1997; Shulman *et al.*, 1998). Studies of the cyto- and myeloarchitecture of the visual cortex have identified V5 within the ITS, within the dorsal arm of the ITS (ALITS) (Tootell and Taylor, 1995) and on the lateral occipital gyri specifically in the lateral (occipital) sulcus (Clarke and Miklossy, 1990; Clarke, 1993). These cyto- and myeloarchitectural results are in agreement with our findings. Therefore we conclude that the variability of fMRI responses does not play a significant role in the explanation of our results.

Implications for Brain Imaging

Rademacher *et al.* (Rademacher *et al.*, 1993) found that the prominent variability of 'primary' cytoachitectonical areas is closely predictable from gross anatomical morphology of the brain [see also (Stensaas *et al.*, 1974; Gilissen and Zilles, 1996)]. Based on these observations, Rademacher *et al.* suggested that a direct reference to the landmarks that frame these areas may be a more reliable basis for functional mapping. The stereotaxic space as defined by Talairach and Tournoux (Talairach and Tournoux, 1988) exhibits variations in gross anatomical features (Steinmetz *et al.*, 1989, 1990, 1991; Hunton *et al.*, 1996). Non-linear alignment of gross anatomical structures would reduce this kind of variability (Collins *et al.*, 1996) (Collins *et al.*, submitted for publication). Our results show that, for human area V5, a linear alignment with two possible landmarks did

not improve the alignment of the individual V5 positions. This suggests that even after alignment of gross cortical features, residual variability might still arise from the variability between gross anatomical features and functional areas.

Conclusion

We have used fMRI to determine the precise relationship between the location of human V5 and the sulcal pattern in the parieto-temporo-occipital cortex. Our results confirm the stereotaxic location of V5, describe the sulcal pattern in the region of interest, quantify the variability of V5 in relation to the sulcal pattern and offer a more useful anatomical landmark, i.e. the ITS–ALITS junction, for localizing V5 with respect to gross morphological features on individual cortical surfaces.

References

Anderson SJ, Holliday IE, Singh GD, Harding GFA (1996) Localization and functional analysis of human cortical area V5 using magneto-encephalography. Proc R Soc Lond B 263:423–431.

Barton JJS, Simpson T, Kiriakopoulos E, Stewart C, Crawley A, Gurthrie B, Wood M, Mikulis D (1996) Functional MRI of lateral occipitotemporal cortex during pursuit and motion perception. Ann Neurol 40: 387–398.

Beauchamp MS, Cox RW, DeYoe EA (1997) Graded effects of spatial and featural attention on human area MT and associated motion processing areas. J Neurophysiol 78:516–520.

Brodmann K (1909) Vergleichende lokalisationslehre der grosshirnrinde in ihren prizipien dargestellt auf grund des zellenbaues. Leipzig: Barth.

Carpenter MB (1991) Neuroanatomy. Baltimore, MD: Wiliams & Wilkins.

Casey BJ, Cohen JD, O'Craven K, Davidson RJ, Irwin W, Nelson CA, Noll DC, Hu X, Lowe MJ, Rosen BR, Truwitt CL, Turski PA (1998) Reproducibility of fMRI results across four institutions using a spatial working memory task. NeuroImage 8: 249–261.

Cheng K, Hasegawa T, Saleem KS, Tanaka K, (1994) Comparison of neuronal selectivity for stimulus speed, length, and contrast in the prestrate visual cortical areas V4 and MT of the macaque monkey. J Neurophysiol 71:2269–2280.

Cheng K, Fujita H, Kanno I, Miura S, Tanaka K (1995) Human cortical regions activated by wide-field visual motion: an $H_2^{15}O$ PET study. J Neurophysiol 74:413–427.

Chusid JG (1973) Correlative neuroanatomy & functional neurology. Los Altos, CA: Lange Medical Publications.

Clarke S (1993) Modular organization of human extrastriate cortex: evidence from cytochrome oxidase pattern in normal and macular degeneration cases. Eur J Neurosc 6:725–736.

Clarke S, Miklossy J (1990) Occipital cortex in man: organization of callosal connections, related myelo- and cytoarchitecture, and putative boundaries of functional visual areas. J Comp Neurol 298: 188–214.

Collins DL, Neelin P, Peters TM, Evans AC (1994) Automatic 3D

intersubject registration of MR volumetric data in standardized Talairach space. J Comput Assist Tomogr 18:192–205.

Collins DL, Le Goualher G, Venugopal R, Caramanos Z, Evans A, Barillot C (1996) Cortical constraints for non-linear cortical registration. Proc Visual Biomed Comput 307–316.

DeArmond SJ, Fusco MM, Dewey MM (1989) Structure of the human brain. A photographic atlas. New York: Oxford University Press.

DeGroot J (1991) Correlative neuroanatomy. Norwalk, UT: Appleton & Lange.

De Jong BM, Shipp S, Skidmore B, Frackowiak RSJ, Zeki S (1994) The cerebral activity related to the visual perception of forward motion in depth. Brain 117:1039–1054.

Dettmers C, Connelly A, Stephan KM, Turner R, Friston KJ, Frackowiak RSJ, Gadian DG (1996) Quantitative comparison of functional magnetic resonance imaging with positron emmission tomography using a force-related paradigm. NeuroImage 4:201–209.

DeYoe EA, Van Essen DC (1988) Concurrent processing streams in monkey visual cortex. Trends Neurosci 11:219–226.

DeYoe EA, Carman GJ, Bandettini P, Glickman S, Wieser J, Cox R, Miller D, Neitz J (1996) Mapping striate and extrastriate visual areas in human cerebral cortex. Proc Natl Acad Sci USA 93:2383–2386.

Dupont P, Orban GA, De Bruyn B, Verbruggen A, Mortelmans L (1994) Many areas in the human brain respond to visual motion. J Neurophysiol 72:1420–1424.

Duvernoy HM (1991) The human brain. Surface, 3-D sectional anatomy and MRI. New York: Springer-Verlag.

Engel SA, Glover GH, Wandell BA (1997) Retinotopic organization in human visual cortex and the spatial precision of functional MRI. Cereb Cortex 7:181–192.

Evans AC, Collins DL, Milner B (1992) An MRI-based stereotaxic atlas from 250 young normal subjects. Soc Neurosci Abstr 18:408.

Freitag P, Greenlee MW, Lacina T, Scheffler K, Radü EW (1998) Effect of eye movements on the magnitude of functional magnetic resonance imaging responses in extrastriate cortex during visual motion perception. Exp Brain Res 119:409–414.

Gilissen E, Zilles K (1996) The calcarine sulcus as an estimate of the total volume of the human striate cortex: a morphometric study of reliability and intersubject variability. J Brain Res 37:57–66.

Hasnain MK, Fox PT, Woldorff MG (1998) Intersubject variability of functional areas in the human visual cortex. Hum Brain Map 6:301–315.

Howard RJ, Bullmore E, Brammer M, Williams SCR, Mellers J, Woodruff P, David A, Andrew C, Allin M, Simmons A, Cox T (1995) Activation of area V5 by visual perception of motion demonstrated with echoplanar MR imaging. Magn Res Imag 13:907–909.

Hunton DL, Miezin FM, Buckner RL, Van Mier HI, Raichle ME, Petersen SE (1996) An assessment of functional–anatomical variability in neuroimaging studies. Hum Brain Map 4:122–139.

Jiang A, Kennedy DN, Baker JR, Weiskoff RM, Tootell RBH, Woods RP, Benson RR, Kwong KK, Brady TJ, Rosen BR, Belliveau JW (1995) Motion detection and correction in functional MR imaging. Hum Brain Map 3:224–235.

Lagae L, Maes H, Raiguel S, Xiao D-K, Orban GA (1994) Responses of macaque STS neurons to optic flow components: a comparison of areas MT and MST. J Neurophysiol 71:1597–1626.

Le Goualher G, Barillot C, Bizais Y, Scarabin J-M (1996) 3D segmentation of cortical sulci using active models. Proceedings of Medical Imaging. SPIE Med Imag 2710:254–564.

Le Goualher G, Procyk E, Collins L, Petrides M, Evans AC (1998) Sulcus extraction and automatic labelling (SEAL): I. Mapping of sulcal neuroanatomy. NeuroImage 7:S729.

McCarthy G, Spicer M, Adrignolo A, Luby M, Gore J, Allison T (1995) Brain activation associated with visual motion studied by functional magnetic resonance imaging in humans. Hum Brain Map 2:234–243.

MacDonald JD (1996) Display: a user's manual. Montreal: McConnel Brain Imaging Centre, Montreal Neurological Institute.

MacDonald JD (1998) A method for identifying geometrically simple surfaces from three dimensional images. PhD dissertation, McGill University.

MacDonald JD, Avis D, Evans AC (1994) Multiple surface identification and matching in magnetic resonance images. Proc Visual Biomed Comput 160–169.

MacDonald JD, Avis D, Evans AC (1998) Automatic segmentation of surfaces from MRI with partial-volume correction. NeuroImage 7:S703.

Maes F, Collignon A, Vandermeulen D, Marchal G, Suetens P (1997) Multi-modality image registration by maximization of mutual information. IEEE Trans Med Imag 16:187–198.

Maunsell JHR, Nealey TA, DePriest DD (1990) Magnocellular and parvocellular contributions to responses in the middle temporal area (MT) of the macaque monkey. J Neurosci 10:3323–3334.

Nolte J (1999) The human brain. An introduction to its functional anatomy. St Louis, MO: Mosby.

O'Craven KM, Rosen BR, Kwong KK, Treisman A, Savoy RL (1997) Voluntary attention modulates fMRI activity in human MT-MST. Neuron 18:591–598.

Ono M, Kubic S, Abernathey CD (1990) Atlas of the cerebral sulci. Stuttgart: Thieme.

Pelli DG (1997) The video toolbox software for visual psychophysics: transforming numbers into movies. Spatial Vis 10:437–442.

Rademacher J, Caviness VS Jr, Steinmetz H, Galaburda AM (1993) Topographical variations of the human primary cortices: implications for neuroimaging, brain mapping, and neurobiology. Cereb Cortex 3:313–329.

Ramsey NF, Kirkby BS, Van Gelderen P, Berman KF, Duyn JH, Frank JA, Mattay VS, Van Horn JD, Esposito G, Moonen CTW, Weinberger DR (1996a) Functional mapping of human sensorimotor cortex with 3D BOLD fMRI correlates highly with $H_2^{15}O$ PET rCBF J Cereb Blood Flow Metab 16:755–764.

Ramsey NF, Tallent K, Van Gelderen P, Frank JA, Moonen CTW, Weinberger DR (1996b) Reproducibility of human 3D fMRI brain maps acquired during a motor task. Hum Brain Map 4:113–121.

Roland PE, Zilles K (1998) Structural divisions and functional fields in the human cerebral cortex. Brain Res Rev 26:87–105.

Ramsey NF, Kirkby BS, Van Gelderen P, Berman KF, Duyn JH, Frank JA,

Sclar G, Maunsell JHR, Lennie P (1990) Coding of image contrast in central visual pathways of the macaque monkey. Vis Res 30:1–10.

Sereno M, Dale A, Reppas J, Kwong K, Belliveau J, Brady T, Rosen B, Tootell R (1995) Borders of multiple visual areas in humans revealed by functional magnetic resonance imaging. Science 268:889–893.

Shulman GL, Schwarz J, Miezin FM, Petersen SE (1998) Effect of motion contrast on human cortical responses to moving stimuli. J Neurophysiol 79:2794–2803.

Sled JG, Zijdenbos AP, Evans AC (1998) A non-parametric method for automatic correction of intensity non-uniformity in MRI data. IEEE Trans Med Imag 17:87–97.

Steinmetz H, Fürst G, Freund H-J (1989) Cerebral cortical localization: application and validation of the proportional grid system in MR imaging. J Comput Assist Tomogr 13:10–19.

Steinmetz H, Fürst G, Freund H-J (1990) Variation of perisylvian and calcarine anatomic landmarks within stereotaxic proportional coordinates. Am J Neuroradiol 11:1123–1130.

Steinmetz H, Fürst G, Freund H-J (1991) Functional anatomy of language processing: neuroimaging and the problem of individual variability. Neuropschologia 29:1149–1161.

Stensaas SS, Eddington DK, Dobelle WH (1974) The topography and variability of the primary visual cortex in man. J Neurosurg 40:747–755.

Talairach J, Tournoux P (1988) Co-planar stereotaxic atlas of the human brain. New York: Thieme.

Tootell RBH, Taylor JB (1995) Anatomical evidence for MT and additional cortical visual areas in humans. Cereb Cortex 1:39–55.

Tootell RBH, Reppas JB, Kwong KK, Malach R, Born RT, Brady TJ, Rosen BR, Belliveau JW (1995) Functional analysis of human MT and related visual cortical areas using functional magnetic resonance imaging. J Neurosci 15:3215–3230.

Tootell RBH, Dale AM, Sereno MI, Malach R (1996) New images from human visual cortex. Trends Neurosci 19:481–489.

Tootell RBH, Mendola JD, Hadjikhani NK Ledden PJ, Liu AK, Sereno MI, Dale AM (1997) Functional analysis of V3A and related areas in human visual cortex. J Neurosci 17:7060–7078.

Uusitalo MA, Jousmäki V, Hari R (1997) Activation trace lifetime of human cortical responses evoked by apparent visual motion. Neurosci Lett 224:45–48.

Watson JDG, Myers R, Frackowiak RSJ, Hajnal JV, Woods RP, Mazziota JC, Shipp S, Zeki S (1993) Area V5 of the human brain: evidence from a combined study using positron emission tomography and magnetic resonance imaging. Cereb Cortex 3:79–94.

Woods RP, Cherry SR, Mazziotta JC (1992) Rapid automated algorithm for aligning and reslicing PET images. J Comput Assist Tomogr 16:620–633.

Woods RP, Grafton ST, Holmes CJ, Cherry SR, Mazziotta JC (1998) Automated image registration: I. General methods and intrasubject, intramodality validation. J Comput Assist Tomogr 22:141–154.

Zeki S, Watson JDG, Lueck CJ, Friston KJ, Kennard C, Frackowiak RSJ (1991) A direct demonstration of functional specialization in human visual cortex. J Neurosci 11:641–649.

Zilles K, Armstrong E, Schleicher A Kretschmann H-J (1988) The human pattern of gyrification in the cerebral cortex. Anat Embryol 179:173–179.